Latin American Journal of Aquatic Research, 54(3): 344-357, 2026
DOI: 10.3856/vol54-issue3-fulltext-3566

Research Article

ENSO-linked catch anomalies and stock status of the *Scomberomorus* genus in northwestern Mexico

Marcelino Ruiz-Domínguez[1], Marlenne Manzano-Sarabia[1] Jorge Saul Ramirez-Perez[1] Casimiro Quiñonez-Velazquez[2] & Concepcion Enciso-Enciso[3]

[1]Facultad de Ciencias del Mar, Universidad Autónoma de Sinaloa, Mazatlán, Sinaloa, México
[2]Instituto Politécnico Nacional, Centro Interdisciplinario de Ciencias Marinas
La Paz, Baja California Sur, México
[3]Instituto Mexicano de Investigación en Pesca y Acuacultura Sustentables
Centro Regional de Investigación Pesquera, Ensenada, Baja California, México
Corresponding author: Marcelino Ruiz-Domínguez (marcelinoruizdom@uas.edu.mx)

ABSTRACT. Species of the genus *Scomberomorus* (*S. sierra* and *S. concolor*) are key resources for artisanal fisheries along the Mexican Pacific coast, with annual catches exceeding 25,000 t. However, information on their population dynamics, responses to ocean-atmospheric variability, and stock assessment remains limited. To address this gap, we analyzed 175,750 landing records alongside monthly Oceanic Niño Index (ONI) data. Temporal catch patterns were evaluated using sequential regime shift analysis (STARS). *S. sierra* exhibited two regimes: a relatively stable phase from 2000 to 2015, followed by elevated catches from 2016 to 2022, whereas *S. concolor* displayed three shifts: low catches (2000-2007), increased catches (2008-2021), and a marked increase in 2022. Cross-correlation function (CCF) analysis revealed contrasting responses to ONI, with *S. sierra* showing a positive relationship ($r = 0.37$, $P = 0.04$) and *S. concolor* showing a negative one ($r = -0.40$, $P = 0.009$). Stock status assessed using the catch maximum sustainable yield (CMSY) model. For *S. sierra*, the estimated maximum sustainable yield (MSY) was 4,873 t, the biomass at MSY (BMSY) was 14,144 t, and the fishing mortality at MSY (F_{MSY}) was 0.34. Historical catches were generally sustainable, but recent increases create potential risks if they continue. For *S. concolor*, MSY was estimated at 5,951 t, BMSY was 17,275 t, and F_{MSY} was 0.34; catches largely remained within sustainable limits, despite slightly exceeding MSY in 2022. Kobe plot analyses indicate *S. sierra* is approaching "overexploitation", whereas *S. concolor* remains within optimal limits. Highlight the need for active management strategies to ensure long-term sustainability.

Keywords: *Scomberomorus*; catch anomalies; stock assessment; Oceanic Niño Index (ONI); CMSY

INTRODUCTION

The genus *Scomberomorus* belongs to the Scombridae family, which includes 16 species in the Mexican Pacific Ocean (Robertson & Allen 2015), nearly all of which serve as commercial, recreational, and/or coastal fishery resources. The Pacific sierra, *S. sierra*, and the gulf sierra, *S. concolor*, constitute a significant portion of the artisanal fishing catch. At the same time, their other congeners, such as bonitos, mackerels, and tuna, are targeted by different fleets (sport fishing and offshore fisheries).

Species of the *Scomberomorus* genus are commonly referred to as "sierras" and inhabit coastal waters (neritic zones). Most undertake substantial seasonal migrations associated with feeding and reproduction

Associate Editor: Yassir Torres

(Collette & Nauen 1983). Due to their seasonal availability, they are considered opportunistic resources (Ramírez-Pérez 2010), particularly from November to July, when other economically valuable resources (e.g. shrimp) are either under fishing bans or experiencing a poor fishing season (Arámburo-Paéz et al. 1984, Montemayor-López & Cisneros-Mata 2000, Cervantes-Escobar 2004, Medina-Gómez 2004). Sierras are highly valued in both the national and international markets. Owing to their nutritional benefits, sierra is considered one of the most attractive species for consumers along the Mexican coast (Montemayor-López & Cisneros-Mata 2000). Annual catches of up to 25,166 t have been reported, and the resource currently ranks 14th in capture volume and 17th in economic value at the national level (SAGARPA 2021). The fishing methods used for these species include seine or gill nets measuring 400, 600, and 800 m in length, with 150 and 200 meshes in height and mesh sizes ranging from 63.5-76.2 mm (2.5-3 inches). Trolling lines are also used as an alternative fishing method (Arámburo-Páez et al. 1984, Lizárraga-Rodríguez 1984, INP 2001).

However, as with many other coastal resources, Sierra is a commercially important species for which studies on population dynamics remain limited (Nava-Ortega et al. 2012). Consequently, biomass estimates are needed to understand the status of the resource and to design active fisheries management measures. Therefore, the objective of this study was to assess the "sierra" resources along the Mexican Pacific coast by estimating biological reference points (BRPs) and proposing an adaptive management approach based on active regulatory measures, such as catch quotas. The findings could provide insights into the current state of this resource and support sustainable socioeconomic fishing practices for the foreseeable future.

MATERIALS AND METHODS

Catch data

Fishery statistics from landing logbooks of the small-scale fishery on the Mexican Pacific coast were available for the period 2000 to 2022. These data were obtained from the fisheries offices of Mexico's Ministry of Agriculture and Rural Development (Secretaría de Agricultura y Desarrollo Rural - SADER). The 23-year series comprises 169,002 catch records. Corresponding to 10 states along the Mexican Pacific coast (Fig. 1): Baja California Sur (n = 13,666), Baja California (n = 5,745), Sonora (n = 14,407), Sinaloa (n = 42,423), Nayarit (n = 37,212), Jalisco (n = 13,636), Colima (n = 6,148), Michoacán (n = 8,397), Guerrero (n = 16,142), and Oaxaca (n = 11,226). In Mexico, official catch records do not distinguish between *S. sierra* and *S. concolor*; both species are recorded simply as "sierra" due to their morphological similarities and the use of similar fishing gear. However, in this study, we separated the catch data based on the landing locations recorded in the landing logbooks, following the literature that defines the distribution area of each species, as well as input from researchers and officials familiar with these resources (Fitch & Flesching 1949, Collette 1995, Aguirre-Villaseñor et al. 2006, Valdovinos-Jacobo 2006, Lucano-Ramirez et al. 2011, Dominguez-Lopez et al. 2015, Ramírez-Pérez et al. 2015, Roberton & Allen 2015, Magallón-Gayon et al. 2016); therefore, the catches were separated latitudinally. In this context, all records obtained south of the major islands of the Gulf of California (Angel de la Guarda Island and Tiburón Island) and extending to the coast of Oaxaca correspond to *S. sierra* (n = 153,926). In contrast, all those obtained north of these islands were attributed to *S. concolor* (n = 15,076). A sequential *t*-test analysis of regime shift (STARS) developed by Rodionov (2004) was applied to detect step changes in the catch time series. STARS uses a *t*-test to determine whether sequential observations in a time series represent statistically significant departures from the mean values observed during a predetermined prior period. El Niño years lead to low productivity in the Gulf of California, reducing fisheries productivity (Santamaria-del-Ángel et al. 1994, Valdovinos-Jacobo 2006). The relationships among the annual catch anomalies of *S. sierra* and *S. concolor* and El Niño-Southern Oscillation (ENSO) events were assessed using cross-correlation function (CCF) analyses (Alves et al. 2021). Monthly ENSO data from 2000 to 2022 were obtained from the National Oceanic and Atmospheric Administration (NOAA 2024). Annual catch anomalies were calculated as follows: $C_{Anom_i} = (C_{ij} - C_{AvrTotal_i}) / C_{AvrTotal_i}$, where C_{Anom_i} is the annual catch anomaly per species (i = *S. sierra*, *S. concolor*), C_{ji} is the catch of species i in year j, and $C_{AvrTotal_i}$ is the average catch for species i over the entire period. The temporal trend of catch anomalies was described by fitting a fifth-order polynomial model (Cárdenas-Quintana et al. 2015).

Biomass estimate and fishery reference points

The catch maximum sustainable yield (CMSY) method was used to estimate biomass from catch data and to derive target reference points (MSY, B_{MSY}, and F_{MSY}). In addition to annual catch data, the model requires prior information in addition to annual catch data to

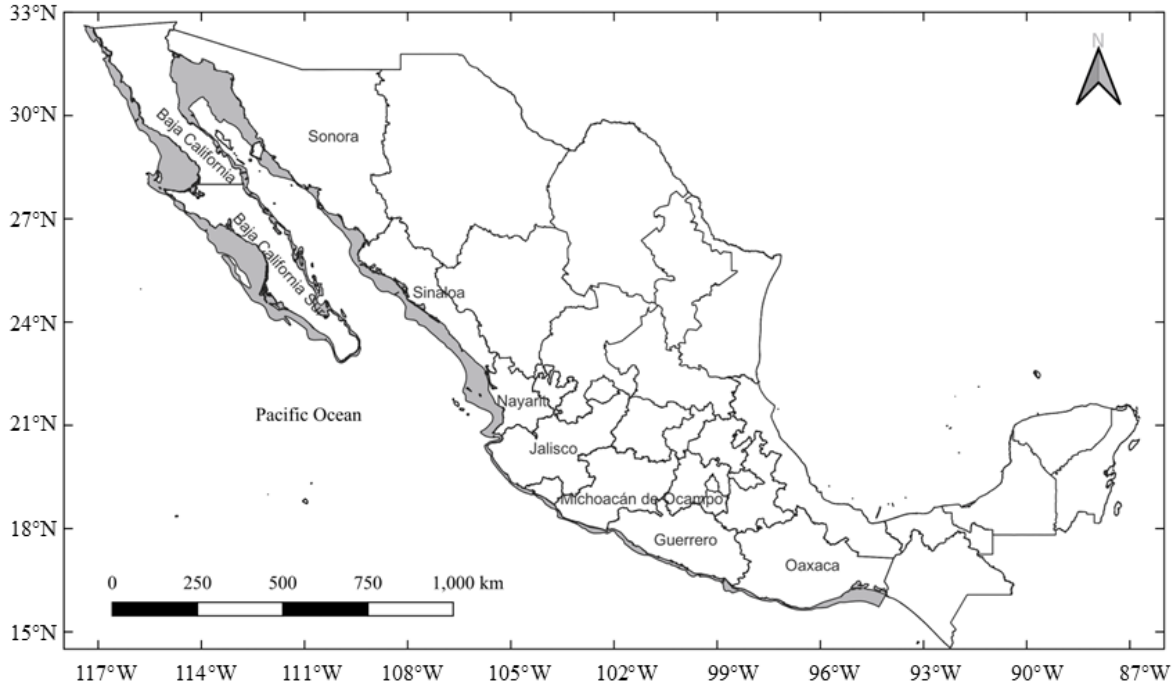

Figure 1. Spatial extent of artisanal fishing operations targeting *Scomberomorus* species in northwestern Mexico.

perform the estimates, including: (1) r, resilience, (2) λ_{001}-λ_{002}, the level of stock depletion in the first year of the time series, (3) λ_{01}-λ_{02}, the level of stock depletion in an intermediate year of the time series, (4) λ_1-λ_2, the level of stock depletion in the last year of the time series, and (5) K, carrying capacity. The information used to parameterize the model is presented in Table 1.

Recommendations by Froese et al. (2017) were followed to define depletion levels for the initial (λ_{001}-λ_{002}), intermediate (λ_{01}-λ_{02}), and final (λ_1-λ_2) years of the time series. Values of r were obtained from records in FishBase (Froese & Pauly 2022) exclusively for *S. sierra*, which was selected as the representative species of the genus due to greater information availability. The K interval was estimated from catch data and resilience, accounting for the depletion level in the final year of the time series (λ_1-λ_2). When λ_1-λ_2<0.5 was assumed, Equation 1 was applied; when λ_1-λ_2>0.5, Equation 2 was applied:

$$K_{low} = \frac{maxC}{r_{high}}, K_{high} = \frac{4(maxC)}{r_{low}} \quad (1)$$

$$K_{low} = \frac{2(maxC)}{r_{high}}, K_{high} = \frac{12(maxC)}{r_{low}} \quad (2)$$

The CMSY is based on two equations. The first corresponds to Schaefer's (1954) surplus production model, which describes population dynamics as a function of biomass growth and fishing mortality (Eq. 3):

$$B_{t+1} = \left[B_t + rB_t\left(\frac{B_t}{K}\right) - C_t\right] \quad (3)$$

where B_{t+1} is the exploited biomass in the subsequent year t_{+1} and in consecutive years of the time series, B_t is the biomass in year t, C_t is the catch in year t, r is the intrinsic rate of population growth, and K is the carrying capacity of the habitat for the stock.

The second equation is applied when if biomass falls below ¼ K. According to Froese et al. (2017), it accounts for depensation or reduced recruitment at severely depleted stock sizes, as predicted by common stock-recruitment functions (Beverton & Holt 1957, Ricker 1975, Barrowman & Myers 2000), and for a linear decline in surplus production, which is a function of recruitment, somatic growth, and natural mortality (Schnute & Richards 2002) (Eq. 4).

$$B_{t+1} = B_t + 4\frac{B_t}{K} r\left(1 - \frac{B_t}{K}\right) B_t - C_t \left|\frac{B_t}{K} < 0.25.\right. \quad (4)$$

The term 4 B_t/K represents a linear decline in recruitment when biomass falls below half the biomass required to produce MSY; the parameters have the same meaning as in Equation 3.

Once all model parameters are obtained, annual estimates of exploitable biomass are derived using Equations 3 and 4. Each simulation uses a different r-K

Table 1. Parameterization data for the catch maximum sustainable yield (CMSY) model for sierras exploited by the artisanal fishery along the Mexican Pacific coast.

	r/a^{-1} (FishBase)	λ_{001}-λ_{002}	intermediate year	λ_{01}-λ_{02}	λ_1-λ_2
S. sierra	0.37-0.85	0.2-0.6	2019	0.2-0.6	0.5-0.9
S. concolor			2020	0.5-0.9	

pair value from the interval ranges presented in Table 1. The viability of each (r-K pair) and the resulting biomass estimates were evaluated under the following three conditions $V(r, K)$; pairs that did not meet these conditions were discarded from the analysis:

The stock does not collapse before the final year of the catch series (Eq. 5). The estimated biomass for the intermediate year of the catch series falls within the stock reduction range assumed a priori (λ_{01} and λ_{02}) (Eq. 5). The estimated biomass for the final year of the catch series also within the stock reduction range assumed a priori (λ_1 and λ_2) (Eq. 5).

$$V(r, K) = \left\{B_{n+1} > K_{0.01}, \lambda_{001} \leq \frac{B_{n+1}}{K} \leq \lambda_{002}, \lambda_{01} \leq \frac{B_{n+1}}{K} \geq \lambda_{02}, \lambda_1 \leq \frac{B_{n+1}}{K} \leq \lambda_2\right\} \quad (5)$$

Once the simulations were completed, the r-K pairs that satisfied the conditions (Eq. 5) were retained. The mean of the predicted biomass values from all viable r-K pairs was used as the central estimate of biomass, and the 2.5th and 97.5th percentiles of the retained simulations were used to represent the uncertainty bounds (95% interval). Because CMSY uses a Monte Carlo filtering approach rather than formal likelihood maximization, uncertainty intervals were derived from the distribution of accepted simulations rather than from likelihood profiling.

Using these parameters, the following target reference points were estimated based on the density functions of the estimated r and K values.

Biomass at which the maximum sustainable yield is obtained (B_{MSY}):

$$B_{MSY} = \frac{K}{2} \quad (6)$$

Maximum sustainable yield (MSY):

$$MSY = \frac{rK}{4} \quad (7)$$

Fishing mortality at maximum sustainable yield (F_{MSY}):

$$F_{MSY} = \frac{r}{2} \quad (8)$$

The means and the 2.5th and 97.5th percentiles were calculated; the means represent the biomass estimate, while the percentiles define the confidence interval.

Kobe diagram

This diagram was used to analyze the resource's state over time graphically. It comprises four panels with distinct characteristics: (1) full exploitation, (2) decline, (3) overfishing, and (4) recovery (Maunder & Aires-da-Silva 2011). The horizontal axis represents the ratio of estimated exploitable biomass at time *t* to the biomass that produces maximum sustainable yield (B_{MSY}). In contrast, the vertical axis represents fishing pressure, expressed as a reference point, related to fishing effort or fishing mortality that produces maximum sustainable yield (F_{MSY}). These axes define four zones that describe different fishing scenarios, including areas where biological sustainability of the resource can be ensured, high-risk areas indicating that the resource is in critical or severely depleted condition, and a threshold area, in which the resource may be subject to overfishing or exploited beyond safe biological limits (Maunder & Aires-da-Silva 2011, Arrizabalaga et al. 2012, Carvalho et al. 2018).

RESULTS

Catch data

The patterns observed in the data series reflect the availability of fishing resources (Fig. 2). Both species generally exhibit a positive trend in catch over time; however, the *S. concolor* series shows greater variability (CV = 50%) than the *S. sierra* series (CV = 32%). Based on exploratory analyses using STARS, the minimum regime length (L) was set to 5 or 10, the step size (H) to 1, and the significance level (*P*) to 0.05. The STARS analysis of the *S. sierra* time series identified two step shifts: the first from 2000 to 2015 ($\bar{x}$ = 3,293 t, CV = 14%), and the second from 2016 to 2022 ($\bar{x}$ = 5,784 t, CV = 12%). During the first 16 years of the series, interannual variability was low to moderate,

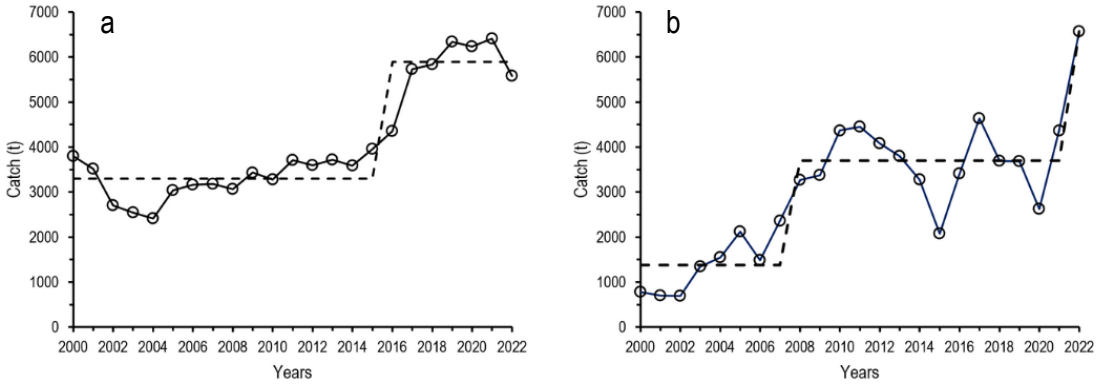

Figure 2. Time series of annual sierra catches along the Mexican Pacific coast, a) *S. sierra* and b) *S. concolor*. Annual values are represented as a solid black line with circles, whereas regime shifts identified using the STARTS method are indicated by dotted black lines.

with minimum and maximum catches of 2,412 and 3,959 t, respectively. The lowest catch recorded during this step was also the lowest across the entire time series. In contrast, the second step shift (2016-2022) was characterized by a sharp increase in annual catches, which rose by an average of 75% compared with the first period, and included the highest catch in the series (6,410 t). For the *S. concolor* catch time series, STARS identified three step shifts: 2000-2007, 2008-2021, and 2022 (Fig. 2b). During the first period ($\bar{x}$ = 1,380 t, CV = 46%), the lowest catches of the entire series were recorded; however, a marked increasing trend was evident, with an average annual increase of 232 t. The second period ($\bar{x}$ = 3,650 t, CV = 20%) was characterized by pronounced interannual variability after 2014, with catches more than doubling between 2015 and 2017, followed by a decline of similar magnitude from 2017 to 2020. The upward trend from 2020 onward continued through 2022, leading STARS to identify the third-step shift that year.

The analysis of the relationships between annual catch anomalies and the ONI generally revealed significant associations. However, while the relationship between Pacific sierra catch anomalies and the ONI was positive (r = 0.37, lag = 3, P = 0.04), whereas it was negative for gulf sierra (r = -0.40, lag = 0, P = 0.009) (Fig. 3). The relatively low catches of Pacific sierra from 2000 to 2014 coincided with predominantly relatively cold ONI conditions, while gulf sierra exhibited a positive trend in annual catches during the same period. This pattern reversed from 2015 to 2021, when temperatures were anomalously warm (2015 ONI = 1.5, the highest value recorded during the study period). Beginning in 2020, ONI anomalies became negative again and persisted through 2022, when an ONI value of -0.9 was recorded, the most negative value of the entire study period. These conditions favored gulf sierra yields, resulting in a historic record catch. A fifth-order polynomial regression model provided a significant description of the temporal trends in catch anomalies for both species.

Biomass estimates and biological reference points (targets and limits)

For *S. sierra*, a total of 1,438 r-K combinations were accepted out of 40,000 simulations, under the three conditions described in the methods section. The selected r and K estimates ranged from 0.37 to 0.85 and from 21,600 to 85,800 t, respectively (Figs. 4a-b). The BRP analysis indicated that MSY ranged from 3,850 to 8,240 t (Fig. 4d), BMSY ranged from 10,800 to 42,900 t (Fig. 4d), and FMSY ranged from 0.185 to 0.425 (Fig. 4e).

For *S. concolor*, 4,890 r-K combinations were accepted from 10,000 simulations. The r and K estimates range from 0.37 to 0.85 and from 15,400 to 120,000 t, respectively (Figs. 5a-b). The estimated MSY from 2,920 to 12,200 t (Fig. 5c), B_{MSY} from 7,690 to 60,200 t (Fig. 5d), and the F_{MSY} from 0.185 to 0.425 (Fig. 5e).

The position of the estimated reference points for both species (*S. sierra* and *S. concolor*) is presented in Table 2. In fisheries management, the mean of each estimate is considered the BRP, while the associated percentiles are interpreted as confidence intervals.

When comparing the annual yields with MSY estimates and their associated confidence intervals for both species, we found that for *S. sierra* (Fig. 6a), mean catches between 2000 and 2016 ($\bar{x}$ = 3,355.28 t) were

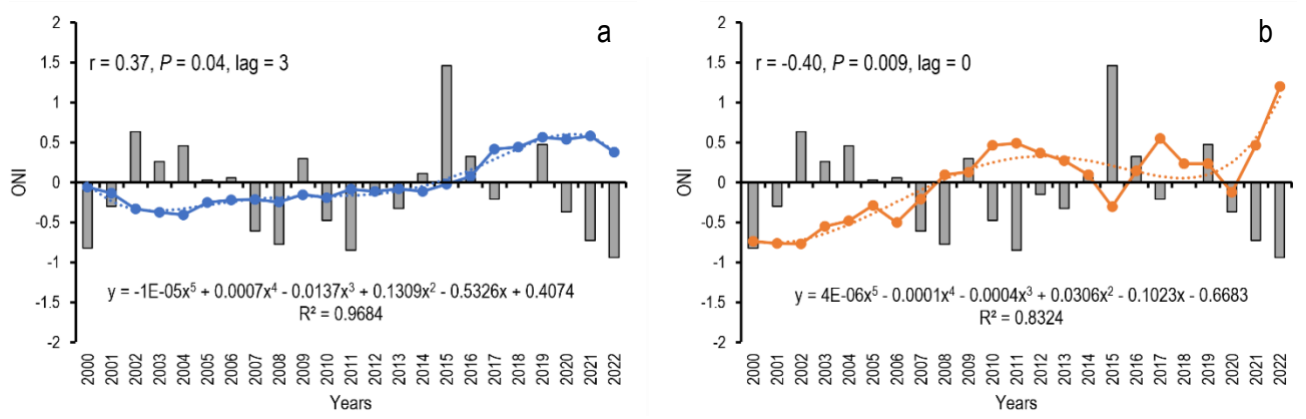

Figure 3. Cross-correlations between annual catch anomalies of sierras along the Mexican Pacific coast. a) *S. sierra* and b) *S. concolor*, and the Oceanic Niño Index (ONI).

below the lower MSY estimate. From 2017 to 2022 ($\bar{x}$ = 6,023.21 t), the catches increased, and on average, they fluctuated around the upper MSY estimate. These results suggest that fishery yields were generally appropriate over much of the time series, remaining within levels consistent with the resource's productive capacity. However, the increase in catches, although still within the upper MSY interval, may affect the resource's stock stability if they continue to rise.

For *S. concolor* (Fig. 6c), fishery yields appear to be in a favorable condition; only in 2022 (the final year of the catch series) did catches exceed the MSY estimate. Under these conditions, current catch levels are likely to be sustainable, provided they do not exceed MSY in subsequent years.

The analysis of historical trends in exploitable biomass (EB) for both species revealed relatively low abundance at the start of the time series. In the case of *S. sierra*, estimated biomass shifted from low values at the start of the series (11,417 t in 2000) to substantially higher values in subsequent years (21,676 t in 2010), before declining again toward the end of the analyzed period (14,144 t in 2022). This pattern may suggest cyclical variability in the stock. However, based on the available information, exploitable biomass has declined markedly in recent years, from 19,967 t in 2017 to 14,144 t in 2022, a 41% reduction. If this trend persists, the stock may approach conditions indicative of overexploitation (EB < B_{MSY}) in the coming years (Fig. 6b). In contrast, *S. concolor* exhibited a different pattern. Although exploitable biomass was also low at the beginning of the time series, abundance increased rapidly thereafter, transitioning from the lowest to the highest levels within approximately six years (2000-2005). Since then, exploitable biomass has fluctuated between 24,980 and 31,641 t and, to date, has shown no evidence of decline. Instead, biomass appears relatively stable, remaining within the upper confidence interval of B_{MSY} (Fig. 6d).

Kobe diagram

Both resources exhibit distinct dynamics. *S. sierra* (Fig. 7a) shows a cyclical pattern; over the 23-year time series analyzed, the stock has transitioned through three of the four quadrants of the Kobe plot. From 2000 to 2002, the stock was in the recovery quadrant. Between 2003 and 2018, it remained in the fully exploited quadrant. Finally, from 2019 to 2022, it shifted into the declining quadrant. This most recent transition from full exploitation to decline coincides with the period in which catches exceeded the upper confidence limit of the estimated MSY. In contrast, *S. concolor* (Fig. 7b) occupied the recovery quadrant only in the first year of the analyzed time series. For the subsequent 22 years (2001-2022), the stock remained within the full exploitation quadrant, which is generally considered the desired condition for a managed fishery. Although some fluctuations occurred within this same quadrant, their magnitude was insufficient to cause a transition to another condition. Thus, the stock has remained fully exploited, meaning it has been maintained near its optimal level.

DISCUSION

Catch data

The catch time series for both species (*S. sierra* and *S. concolor*) reflect a relative index of abundance influenced by both fishing effort and population abundance. A significant relationship was detected between

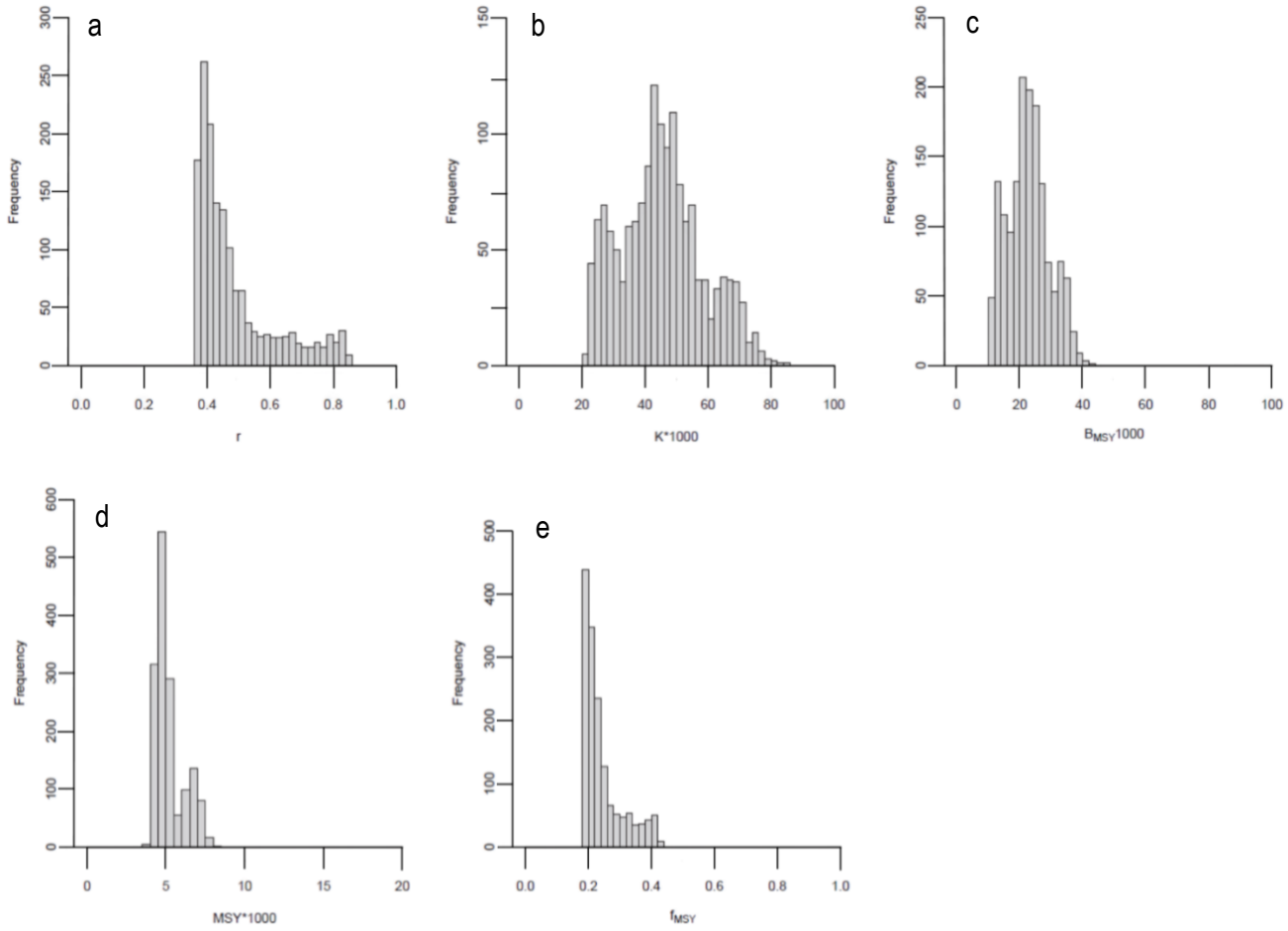

Figure 4. Simulation of biological reference points estimated from accepted r and K pairs for *S. sierra* captured by the coastal fleet along the Mexican Pacific coast. a) Frequency distribution of the intrinsic rate of population increases r, b) carrying capacity K, c) biomass at MSY (B_{MSY}), d) maximum sustainable yield (MSY), and e) fishing mortality at MSY (F_{MSY}).

the catches of the two species (r = 0.55, lag = 0, P = 0.0005). However, evaluating fishing effort separately for each species is challenging because they are only partially exploited within a multispecies fishery. STARS analysis was applied to statistically identify shifts in the catch time series; however, this method has limitations, as it assumes stepwise shifts even when long-term trends change gradually. Two and three distinct stages of fishery development were identified for *S. sierra* and *S. concolor*, respectively. Although the timing of stage transitions differs across species, both exhibit similar overall patterns: low catch levels followed by a significant increase in yields. During the second stage for *S. sierra*, catches increased by up to 180% relative to the first stage, whereas for *S. concolor* the increase reached 278%. These changes were significantly correlated with variations in ONI values; furthermore, the two species exhibited opposite responses to environmental variability.

This semi-synchronous behavior observed in the catches of *S. sierra* and *S. concolor* requires further analysis to identify the mechanisms underlying these similar yet temporally offset patterns. A clearer understanding of the spatial and environmental conditions occupied by each species is therefore required. Although both species are distributed along the eastern Pacific coast of Mexico, *S. sierra* ranges from the southern portion of the large islands in the Gulf of California to the coast of Oaxaca. Three currents primarily influence this region: 1) the California Current, which transports cold water along the Mexican Pacific coast during winter and spring; 2) the North Equatorial Countercurrent, which brings warm waters during summer and autumn; and 3) warm,

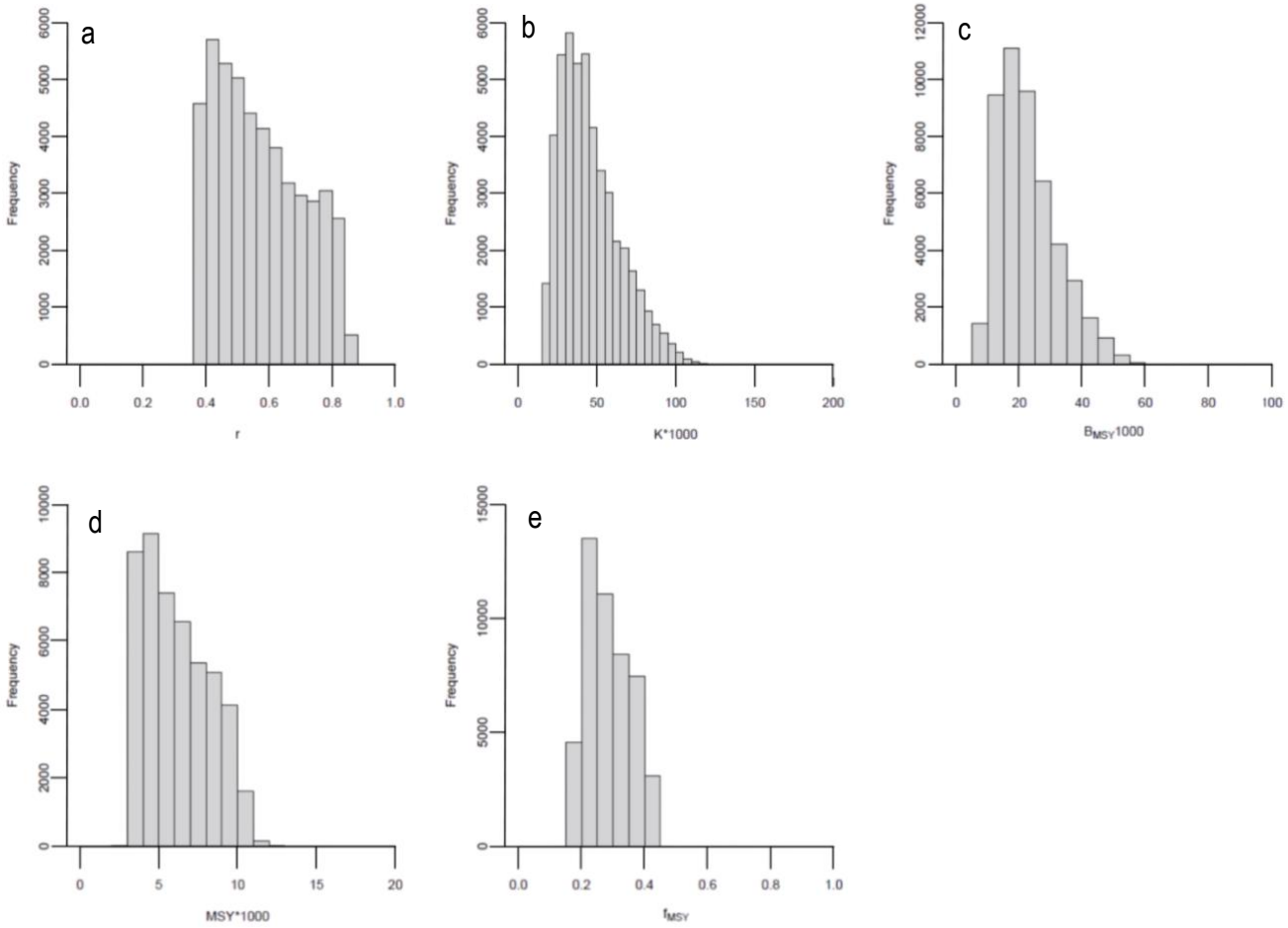

Figure 5. Simulation of biological reference points estimated from accepted r and K pairs for *S. concolor* captured by the coastal fleet fishing off the Mexican Pacific coast. a) Frequency distribution of the intrinsic rate of population increases r, b) carrying capacity K, c) biomass at MSY (B_{MSY}), d) maximum sustainable yield (MSY), and e) fishing mortality at MSY (F_{MSY}).

Table 2. Estimated parameters of the Schaefer's model (1954) model and target reference points for *S. sierra* and *S. concolor* exploited by the coastal fleet fishing along the Mexican Pacific coast.

S. sierra					
BRP	r	K	MSY	B_{MSY}	f_{MSY}
Mean	0.69	28,287	4,873	14,144	0.34
Percentile (2.5%)	0.57	21,003	4,000	10,501	0.28
Percentile (97.5%)	0.84	38,098	5,935	19,049	0.42
S. concolor					
BRP	r	K	MSY	B_{MSY}	f_{MSY}
Mean	0.69	34,549	5,951	17,275	0.34
Percentile (2.5%)	0.57	19,603	2,884	9,801	0.28
Percentile (97.5%)	0.84	60,893	12,281	30,447	0.42

moderately saline water from the eastern tropical Pacific (Aguirre-Gómez 2002). In contrast, *S. concolor* is distributed from the northern portion of the large islands to the Gulf of Santa Clara in the northern Gulf of California, an area dominated by the Gulf of California Current characterized by cold, highly saline

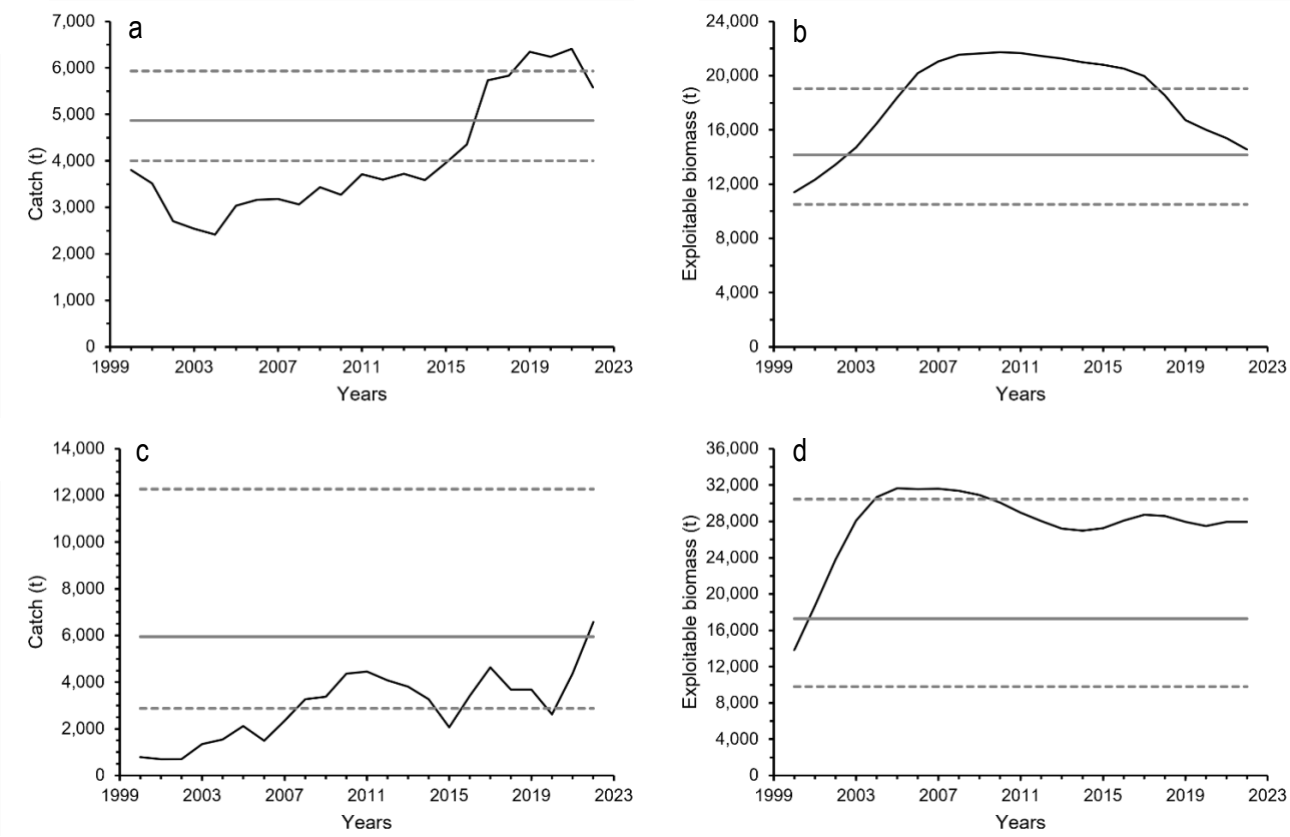

Figure 6. Historical catches series and exploitable biomass for sierra species along the Mexican Pacific coast. a) Historical catch series of *S. sierra* (solid black line), maximum sustainable yield (MSY; solid gray line), and confidence intervals (dotted gray lines), b) historical series of exploitable biomass of *S. sierra* (solid black line), biomass at MSY ($B_{MSY;}$ solid gray lines), and confidence intervals (dotted gray lines), c) historical catch series of *S. concolor* (solid black line), MSY (solid gray line), and confidence intervals (dotted gray lines), d) historical series of exploitable biomass of *S. concolor* (solid black line), B_{MSY} (solid gray lines), and confidence intervals (dotted gray lines).

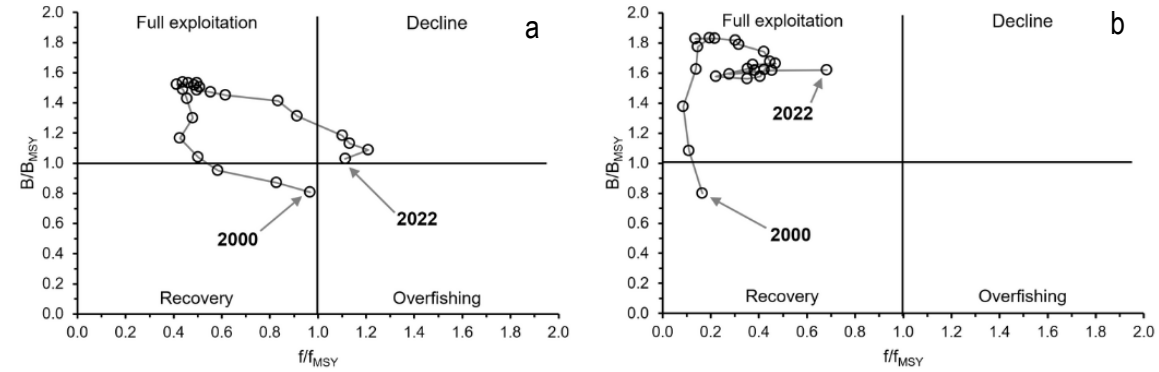

Figure 7. Kobe diagram illustrating historical stock trajectories of sierra species exploited by the artisanal fleet operating along the Mexican Pacific coast. a) *S. sierra* and b) *S. concolor*. B/BMSY represents the ratio of current biomass to the biomass at Maximum Sustainable Yield (MSY), while F/FMSY represents the ratio of current fishing mortality to the fishing mortality at MSY.

waters. During summer, however, the eastern tropical Pacific water mass originating from the southeast penetrates deeply into the gulf, reducing the surface influence of the California Current in this region (Robinson 1973).

The seasonal succession of these marine currents along the western coast of Mexico influences the abundance and/or availability of these species, particularly *S. sierra*. According to Arámburo-Páez et al. (1984), Montemayor-López & Cisneros-Mata (2000), Cervantes-Escobar (2004), Medina-Gómez (2004), and Espino-Barr et al. (2012), the highest catches of Pacific sierra along the Mexican Pacific coast typically occur between October and July.

Historical changes in the catch volumes of both sierra species appear to be closely associated with ENSO variability. The observed pattern indicates that during positive ENSO phases, catches of *S. concolor* declined markedly, whereas during these conditions, catches of *S. sierra* tended to increase. Conversely, under relatively cold conditions (negative ENSO values), the availability of *S. concolor* to the fishery increases substantially. These contrasting responses may be linked to ENSO-induced environmental processes, such as changes in nutrient concentrations within the euphotic zone, upwelling intensity, and sea surface temperature (Swartzman et al. 2008, Su et al. 2011).

The catch responses of *S. sierra* and *S. concolor* to ENSO events have been previously reported for other fishery resources, particularly within the Clupeidae family (e.g. *Sardinops sagax*), for which catches typically decline sharply during positive ENSO phases and remain significantly low in the following years. Gutiérrez-Benítez et al. (2019) reported that ENSO-driven physical changes in the Gulf of California affect phytoplankton biomass, nutrient availability, and primary productivity (Barber & Chávez 1983), thereby modifying spawning environments, larval habitats (Sánchez-Velasco et al. 2004), juvenile recruitment, and ultimately adult availability to fisheries (Hammann et al. 1988). However, not all species respond similarly to ENSO variability; for example, Adams & Flores (2016) observed increased abundance of *Isacia conceptionis* up to two years after a negative ENSO (La Niña) event.

In general, species-specific responses to environmental variability driven by ocean-atmospheric interactions may arise from changes in recruitment dynamics (Cahuin et al. 2009), ecological interactions (Wells et al. 2008), larval and juvenile survival (Alheit & Niquen 2004), reproduction processes (Claramunt et al. 2012), as well as growth and mortality rates (Vilchis et al. 2005). Pauly & Tsukayama (1987), Ñiquen & Bouchon (2004), and Taylor et al. (2008) emphasized that environmental variability typically affects fishery resources at two primary scales: 1) short-term changes in vertical and horizontal distribution that influence availability to fisheries, and 2) longer-term effects on reproduction, recruitment, and biomass.

Estimates of biomass and biological reference points (targets and limits)

The historical EB estimated for both species shows similarities over nearly three-quarters of the analyzed time series. Specifically, from 2000 to 2005, both species exhibited rapid and pronounced increases, reaching values close to the historical maxima of their respective series. During this period, EB increased by 61% for *S. sierra* and by 129% for *S. concolor.* This growth phase was followed by a relatively stable period lasting approximately four years (through 2009), during which EB remained at relatively high levels, with *S. sierra* fluctuating around 21,128 t and *S. concolor* around 31,372 t. After this stable phase, both species entered a period of gradual decline. Notably, EB of *S. sierra* consistently remained above the upper confidence interval (CI) of the BMSY, whereas the EB of *S. concolor* fluctuated below the upper CI of BMSY.

In the most recent portion of the series (post-2017), the two species exhibited markedly divergent dynamics. The EB of *S. sierra* has declined sharply since 2018, approaching the estimated BMSY within five years and maintaining a strong negative trend. If this trend continues, EB may soon fall below this reference point, indicating potential overexploitation. This pronounced shift coincides with catches exceeding the upper CI of MSY, thereby surpassing sustainable yield levels for several consecutive years and potentially constraining stock recovery. Although catches decreased slightly in the final year of the series, the declining EB trend persisted.

In contrast, the EB for *S. concolor* has continued to fluctuate similarly to that observed in the preceding period, with no clear indication of decline. This relative stability appears to be largely associated with catches remaining below the estimated MSY for most of the series. Consequently, exploitation levels for *S. concolor* may be considered well managed. Only in the final year (2022) did catches marginally exceed the estimated MSY; if this represents an isolated event and catches return to lower levels in subsequent years, adverse effects on stock abundance are unlikely.

Ideally, these biomass estimates would be compared with those from other studies conducted along the Mexican Pacific coast; however, such comparative assessments are currently unavailable, as noted in the introduction. Existing studies that provide biological indicators include those by Aguirre-Villaseñor et al. (2006) and Lucano-Ramirez et al. (2011). These authors reported the capture of immature females in *S. sierra* stocks off Mazatlán, Sinaloa, and Barra de Navidad, Jalisco, suggesting the potential for growth overfishing, where excessive numbers of juveniles are harvested (Hilborn & Walters 1992). Aguirre-Villaseñor et al. (2006) emphasized the need for a management strategy that regulates fishing mortality to protect adult spawning biomass. Accordingly, a target fishing mortality rate (FMSY) of 0.34 has been proposed to promote stock sustainability, implying that current fishing mortality levels should be gradually reduced towards this reference point to align exploitation with MSY. Alternatively, an annual catch quota of 4,873 t (the estimated MSY) has been suggested for *S. sierra* along the Mexican Pacific, with a corresponding quota up to 5,951 t for *S. concolor*. These quotas should be allocated proportionally among states exploiting resources, ideally based on relative catch volumes derived from IMIPAS's fisheries statistics (previously named: INAPESCA (Instituto Nacional de Pesca y Acuacultura/National Institute of Fisheries and Aquaculture), landing logs, or the "Sierras" profile in the 2010 version of the National Fisheries Chart (DOF 2010).

Kobe diagram

The Kobe diagram, which illustrates the relationship between relative biomass and relative exploitation rate (Argumedo-Guillen et al. 2021), indicates that both species were in a recovery phase at the beginning of the analyzed time series. Together with the overall patterns observed in the diagram, this suggests cyclical stock dynamics. In the early years, both *S. sierra* and *S. concolor* exhibited market increases in abundance. Subsequently, they fluctuated within the "fully exploited" quadrant, which represents the optimal state for fisheries resources. However, due to elevated catch levels, *S. sierra* transitioned from this quadrant into the "declining" quadrant and is currently approaching the critical "overexploitation" quadrant. Consequently, implementing the previously proposed management measures (e.g. regulating fishing mortality or establishing weighted catch quotas) is essential for this species.

In contrast, *S. concolor* has exhibited favorable conditions from a fishery management perspective, remaining consistently within the "fully exploited" quadrant throughout most of the analyzed period (2001-2022). The only potentially unfavorable signal was a slight shift toward the "declining" quadrant in the final year, likely associated with increased catches. Nonetheless, adopting a precautionary management approach could effectively mitigate this risk and help prevent future stock deterioration.

Finally, an important advantage of the Kobe diagram is its ability to clearly and concisely convey stock assessment results by graphically representing stock status and trajectories across management quadrants over time. This clarity explains why regional fisheries management organizations widely use the Kobe diagram to summarize and communicate stock status effectively (Su et al. 2011).

ACKNOWLEDGMENTS

We thank all those who contributed in any way to the completion of this work. We are also grateful to the Instituto Mexicano de Investigación en Pesca y Acuicultura Sustentable (IMIPAS), which provided the catch data used in this study.

Credit author contribution

M. Ruiz-Domínguez: conceptualization, formal analysis, methodology and writing-original draft; M. Manzano-Sarabia: investigation, validation and writing-review & editing; J.S. Ramirez-Perez: data curation, validation and writing-review & editing; C. Quiñonez-Velazquez: supervision, validation, visualization and writing-review & editing; C. Enciso-Enciso: conceptualization, validation, writing-review and editing.

Conflict of interest

The authors declare that they have no known competing financial interests or personal relationships that could have influenced the work reported in this manuscript. This research did not receive any specific grant from funding agencies in the public, commercial, or not-for-profit sectors.

Data availability

The data supporting the findings of this study are not publicly available due to institutional limitations and the absence of a dedicated repository at the time of research conducted. However, the data are available from the corresponding author upon reasonable request.

REFERENCES

Adams, G.D. & Flores, D. 2016. Influencia de El Niño Oscilación del Sur en la disponibilidad y abundancia de recursos hidrobiológicos de la pesca artesanal en Ica, Perú. Revista de Biología Marina y Oceanografía, 51: 265-272. doi: 10.4067/S0718-19572016000200005

Aguirre-Gómez, R. 2002. Los mares mexicanos a través de la percepción remota. Universidad Nacional Autónoma de México, Ciudad de México.

Aguirre-Villaseñor, H., Morales-Bojórquez, E., Morán-Angulo, R.E., et al. 2006. Indicadores biológicos de la pesquería de sierra (*Scomberomorus sierra*) al sur del Golfo de California, México. Ciencias Marinas, 32: 471-484.

Alheit, J. & Niquen, M. 2004. Regime shifts in the Humboldt Current ecosystem. Progress in Oceanography, 60: 201-222. doi: 10.1016/j.pocean.2004.02.006

Alves, J.C., Andreotti, G.F., Agostinho, A.A., et al. 2021. Effects of the El Niño Southern Oscillation (ENSO) on fish assemblages in a Neotropical floodplain. Hydrobiologia, 848: 1811-1823.

Aramburo-Páez, G., Luna-García, J.M., Tirado-Estrada, G., et al. 1984. Breve estudio sobre la sierra *Scomberomorus sierra*, capturada por pescadores libres de Playa Norte e Isla de la Piedra, Mazatlán. Memorias del Servicio Social, Universidad Autónoma de Sinaloa, Sinaloa.

Argumedo-Guillén, E., Tacuri-Santisteban, P., Pérez-Huaripata, M., et al. 2021. Indicadores biológicos, pesqueros y poblacionales de la lisa *Mugil cephalus* (Linnaeus, 1758) en el litoral peruano. Informe del Instituto del Mar del Perú, 48: 4.

Arrizabalaga, H., Murua, H. & Majkowski, H. 2012. Global status of tuna stocks. Revista de Investigación Marina, 19: 645-676.

Barber, R.T. & Chavez, F.P. 1983. Biological consequences of El Niño. Science, 222: 1203-1210. doi: 10.1126/science.222.4629.1203

Barrowman, N.J. & Myers, R.A. 2000. Still more spawner-recruitment curves: the hockey stick and its generalizations. Canadian Journal of Fisheries and Aquatic Sciences, 57: 665-676. doi: 10.1139/cjfas-57-4-665

Beverton, R.J.H. & Holt, S.J. 1957. On the dynamics of exploited fish populations. Fishery Investigations Ministry of Agriculture, Fisheries and Food, London, 19: 533 pp.

Cahuin, S.M., Cubillos, L.A., Niquen, M., et al. 2009. Climatic regimes and the recruitment rate of anchoveta, *Engraulis ringens*, off Peru. Estuarine, Coastal and Shelf Science, 84: 591-597. doi: 10.1016/j.ecss.2009.07.027

Cárdenas-Quintana, G., Franco-Meléndez, M., Salcedo-Rodríguez, J., et al. 2015. La sardina peruana, *Sardinops sagax*: análisis histórico de la pesquería (1978-2005). Ciencias Marinas, 41: 203-216.

Carvalho, F., Lee, H.H., Piner, K.R., et al. 2018. Can the status of pelagic shark populations be determined using simple fishery indicators? Biological Conservation, 228: 195-204. doi: 10.1016/j.biocon.2018.09.034

Cervantes-Escobar, A. 2004. Variación estacional de la estructura de tallas y madurez gonadal de la sierra del Pacífico *Scomberomorus sierra* en la costa este del Golfo de California. Tesis de Licenciatura, Universidad Autónoma de Sinaloa, Mazatlán.

Claramunt, G., Castro, L.R., Cubillos, L.A., et al. 2012. Interannual reproductive trait variation and spawning habitat preferences of *Engraulis ringens* off northern Chile. Revista de Biología Marina y Oceanografía, 47: 227-243. doi: 10.4067/S0718-19572012000200006

Collette, B.B. 1995. Atunes, bacoretas, bonitos, caballas, estorninos, melva. In: Fischer, W., Krupp, F., Schneider, W., et al. (Eds.). Guía FAO para la identificación de especies para los fines de la pesca. Pacífico centro-oriental, Vol. III. Vertebrados: parte 2. FAO, Rome, pp. 1521-1543.

Collette, B.B. & Nauen, C.E. 1983. Scombrids of the world: An annotated and illustrated catalog of tunas, mackerels, bonitos, and related species known to date. FAO Fisheries Synopsis, 125: 1-137.

Diario Oficial de la Federación (DOF). 2010. Carta Nacional Pesquera. DOF, Ciudad de México.

Domínguez-López, M., Díaz-Jaimes, P., Uribe-Alcocer, M., et al. 2015. Post-glacial population expansion of the Monterey Spanish mackerel *Scomberomorus concolor* in the Gulf of California. Journal of Fish Biology, 86: 1153-1162.

Espino-Barr, E., Nava-Ortega, R.A., Gallardo-Cabello, M., et al. 2012. Aspects of *Scomberomorus sierra* fishery from the coast of Colima, Mexico. Ciencias Pesqueras, 20: 77-88.

Fitch, E.J. & Flesching, A.O. 1949. A brief account of the Monterey Spanish mackerel (*Scomberomorus concolor*). California Fish and Game, 35: 275-280.

Froese, R. & Pauly, D. 2022. FishBase. [www.fishbase.org]. Reviewed: August 22, 2025.

Froese, R., Demirel, N., Coro, G., et al. 2017. Estimating fisheries reference points from catch and resilience. Fish and Fisheries, 18: 506-526.

Gutiérrez-Benítez, O., Galindo-Cortes, G., Velarde-González, E., et al. 2019. Análisis de la serie de captura de sardina Monterrey, *Sardinops sagax* (Jenyns, 1842) en el Golfo de California, México. Hidrobiológica, 29: 83-87. doi: 10.24275/uam/izt/dcbs/hidro/2019v29n2/Gutierrez

Hammann, M.G., Baumgartner, T.R. & Badan-Dangon, A. 1988. Coupling of the Pacific sardine (*Sardinops sagax caeruleus*) life cycle with the Gulf of California pelagic environment. CalCOFI Reports, 29: 102-109.

Hilborn, R. & Walters, C.J. 1992. Stock and recruitment. In: Hilborn, R. & Walters, C.J. (Eds.). Quantitative fisheries stock assessment: Choice, dynamics and uncertainty. Chapman & Hall, New York, pp. 241-296.

Instituto Nacional de la Pesca (INP). 2001. Sustentabilidad y pesca responsable en México: Evaluación y manejo. INP-SAGARPA, Ciudad de México.

Lizárraga-Rodríguez, H.M. 1984. Contribución al conocimiento de las pesquerías de la sierra *Scomberomorus sierra* Jordan y Starks, 1895, en la costa del estado de Nayarit. Memoria de Servicio Social, Universidad Autónoma de Sinaloa, Sinaloa.

Lucano-Ramírez, G., Ruiz-Ramírez, S., Palomera-Sánchez, F.I., et al. 2011. Biología reproductiva de la sierra *Scomberomorus sierra* (Pisces, Scombridae) en el Pacífico central mexicano. Ciencias Marinas, 37: 249-260.

Magallón-Gayón, E., Diaz-Jaimes, P. & Uribe-Alcocer, M. 2016. Spatial and temporal genetic homogeneity of the Monterey Spanish mackerel, *Scomberomorus concolor*, in the Gulf of California. PeerJ, 4: e2583. doi: 10.7717/peerj.2583

Maunder, M.N. & Aires-da-Silva, A. 2011. Evaluation of the Kobe plot and strategy matrix and their application to tuna in the EPO. IATTC Stock Assessment Report, 12: 191-211.

Medina-Gómez, S.P. 2004. Variación estacional de la estructura de tallas y madurez gonadal de *Scomberomorus concolor* (Lockington, 1879) y *Scomberomorus sierra* Jordan y Starks, 1895 en la costa este del Golfo de California, México. Tesis de Licenciatura, Universidad Autónoma de Sinaloa, Sinaloa.

Montemayor-López, G. & Cisneros-Mata, M.A. 2000. La sierra del Golfo de California. In: Sustentabilidad y pesca responsable en México; evaluación y manejo 1997-1998. SEMARNAP-IPN, Ciudad de México, pp. 261-273.

Nava-Ortega, R.A., Espino-Barr, E., Gallardo-Cabello, M., et al. 2012. Growth analysis of the Pacific sierra *Scomberomorus sierra* in Colima, Mexico. Revista de Biología Marina y Oceanografía, 47: 273-281.

National Oceanic and Atmospheric Administration (NOAA). 2024. Oceanic El Niño Index (ONI). [https://origin.cpc.ncep.noaa.gov/products/analysis_monitoring/ensostuff/ONI_v5.php]. Reviewed: 2024.

Ñiquen, M. & Bouchon, M. 2004. Impact of El Niño events on pelagic fisheries in Peruvian waters. Deep-Sea Research Part II, 51: 563-574.

Pauly, D. & Tsukayama, I. 1987. On the implementation of management-oriented fishery research: the case of the Peruvian anchoveta. In: Pauly, D. & Tsukayama, I. (Eds.). The Peruvian anchoveta and its upwelling ecosystem: three decades of change. ICLARM Studies and Reviews, 15: 1-13.

Ramírez-Pérez, J.S. 2010. Estructura poblacional de la sierra del Pacífico *Scomberomorus sierra* Jordan y Starks, 1895 (Perciformes: Scombridae) en el Pacífico mexicano. Doctoral Dissertation, Instituto Politécnico Nacional, La Paz.

Ramírez-Pérez, J.S., García-Rodríguez, F.J., Quiñonez-Velázquez, C., et al. 2015. Recognizing species from commercial catches: Molecular and morphometric analyses of *Scomberomorus* spp. off the Mexican Pacific Coast. Turkish Journal of Fisheries and Aquatic Sciences, 15: 205-214. doi: 10.4194/1303-2712-v15_2_02

Ricker, W.E. 1975. Computation and interpretation of biological statistics of fish populations. Bulletin of the Fisheries Research Board of Canada, 191: 1-382.

Robertson, D.R. & Allen, G.R. 2015. Peces costeros del Pacífico Oriental Tropical: sistema de información en línea. Versión 2.0. Instituto Smithsonian de Investigaciones Tropicales, Balboa. [https://biogeodb.stri.si.edu/sftep/es/pages]. Reviewed: November 15, 2021.

Robinson, M.K. 1973. Atlas of monthly mean surface and subsurface temperatures in the Gulf of California, Mexico. San Diego Society of Natural History, San Diego.

Rodionov, S.N. 2004. A sequential algorithm for testing climate regime shifts. Geophysical Research Letters, 31: 9. doi: 10.1029/2004GL019448

Secretaría de Agricultura, Ganadería, Desarrollo Rural, Pesca y Alimentacion (SAGARPA). 2021. Anuario estadístico de acuacultura y pesca 2021. Comisión Nacional de Acuacultura y Pesca, Mazatlán.

Sánchez-Velasco, L., Avalos-García, C., Rentería-Cano, M., et al. 2004. Fish larvae abundance and distribution in the central Gulf of California during strong environmental changes (1997-1998 El Niño and 1998-1999 La Niña). Deep-Sea Research Part II, 51: 711-722. doi: 10.1016/j.dsr2.2004.05.021

Santamaría-del-Ángel, E., Álvarez-Borrego, S. & Muller-Karger, F. 1994. Gulf of California biogeographic regions based on coastal zone color scanner imagery. Journal of Geophysical Research, 99: 7411-7421.

Schaefer, M.B. 1954. Some aspects of the dynamics of populations important to the management of the commercial marine fisheries. Inter-American Tropical Tuna Commission Bulletin, 1: 23-56.

Schnute, J.T. & Richards, L.J. 2002. Surplus production models. In: Hart, P.J.B. & Reynolds, J.D. (Eds.). Handbook of fish biology and fisheries. Blackwell, Oxford, 2: 105-126. doi: 10.1017/S037689290325 0414

Su, N.J., Sun, C.L., Punt, A.E., et al. 2011. Modelling the impacts of environmental variation on the distribution of blue marlin, *Makaira nigricans*, in the Pacific Ocean. ICES Journal of Marine Science, 68: 1072-1080.

Swartzman, G., Bertrand, A., Gutiérrez, M., et al. 2008. The relationship of anchovy and sardine to water masses in the Peruvian Humboldt Current System from 1983 to 2005. Progress in Oceanography, 79: 228-237. doi: 10.1016/j.pocean.2008.10.021

Taylor, M.H., Wolff, M., Mendo, J., et al. 2008. Changes in trophic flow structure of Independence Bay (Peru) over an ENSO cycle. Progress in Oceanography, 79: 336-351. doi: 10.1016/j.pocean.2008.10.006

Valdovinos-Jacobo, A.L. 2006. Edad, crecimiento y mortalidad de la sierra del golfo *Scomberomorus concolor* (Lockington, 1879) en el Golfo de California. Doctoral Dissertation, Instituto Politécnico Nacional, La Paz.

Vilchis, L.I., Tegner, M.J., Moore, J.D., et al. 2005. Ocean warming effects on growth, reproduction, and survivorship of southern California abalone. Ecological Applications, 15: 469-480. doi: 10.1890/03-5326

Wells, B.K., Field, J.C., Thayer, J.A., et al. 2008. Untangling the relationships among climate, prey, and top predators in an ocean ecosystem. Marine Ecology Progress Series, 364: 15-29. doi: 10.3354/meps07486

Received: November 18, 2025; Accepted: March 17, 2026